Crystal Growth, Structural Characterization, and Linear Thermal Evolution of $KGd(PO_3)_4$

I. Parreu, R. Solé, Jna. Gavaldà, J. Massons, F. Díaz, and M. Aguiló*

Física i Cristallografia de Materials (FiCMA), Universitat Rovira i Virgili, C. Marcel lí Domingo, 43007, Tarragona, Spain

Received September 9, 2004. Revised Manuscript Received November 5, 2004

We determined the crystallization region of $KGd(PO_3)_4$ (KGP) in the ternary system $Gd_2O_3-K_2O-P_2O_5$, the isotherms of saturation temperature and six neighboring phases: KPO_3, $GdPO_4$, $KGdP_4O_{12}$, $Gd(PO_3)_3$-orthorhombic, $Gd(PO_3)_3$-monoclinic, and GdP_5O_{14}. We successfully grew KGP single crystals by the top-seeded solution growth (TSSG) slow cooling method. To optimize the growth process and obtain high-quality KGP crystals, solution composition and seed orientation were analyzed and a growth device was added. KGP is isostructural to $KNd(PO_3)_4$, crystallizes in the monoclinic system $P2_1$ and the cell parameters determined are $a = 7.2701(11)$, $b = 8.3818(8)$, and $c = 7.9608(10)$ Å, $\beta = 91.776(12)°$, $Z = 2$, and $V = 484.87(11)$ Å^3. We studied how they evolved as the temperature increased from room temperature to 773 K and observed an almost isotropic linear thermal expansion, the tensor of which we also calculated. In the room temperature to 1273 K range analyzed, we found that KGP irreversibly decomposed at 1142 K. The second harmonic efficiency, qualitatively measured by the Kurtz method, was at least similar to that of KH_2PO_4 (KDP).

Introduction

Condensed phosphates have been widely studied because they can be used in several scientific fields, such as catalysis, electricity, and optics. Optics involves the so-called polyphosphates of lanthanides, which are generated from a large number of phosphate ions in either long-chain or cycling geometry. Several of these are reported[1−11] to have good optical properties for the laser technology field. Most are neodymium-stoichiometric polyphosphates designed for use as mini-lasers, such as $KNd(PO_3)_4$ (KNP).[5,8,12] KNP has two important advantages: first, it can be obtained as high-quality single crystal, and second, its almost isotropic thermal expansion prevents it from deforming.

We therefore decided to grow and study $KGd(PO_3)_4$ (KGP). This material should maintain the good properties of KNP because it is reported to be isostructural[13] to it and, in fact, we verified this by comparing both X-ray powder diffraction patterns recorded in the same conditions. KGP was therefore regarded as a promising new laser host that can also be easily doped with any other lanthanide ion since the gadolinium has a high capacity to be substituted.

In this paper we analyze the conditions of the KGP crystal growth process and present its basic structural characterization.

As KGP has never been reported before, we performed a parallel study to our previous one for KNP,[12] for which there is also little information in the literature. We determined the KGP crystallization region in the self-flux. Then, taking into account the results obtained with KNP, we optimized its crystal growth process. The KGP cell parameters and morphology were determined. We also studied how KGP behaved with temperature and determined thermal expansion and phase transitions. Finally, as this structure is not centrosymmetric, we qualitatively analyzed the possibility of second harmonic generation.

Experimental Section

Crystallization Region of $KGd(PO_3)_4$. To determine the region where $KGd(PO_3)_4$ crystallizes as a single phase in its self-flux, we grew small crystals of a large number of compositions in the $Gd_2O_3-K_2O-P_2O_5$ ternary system and determined their saturation temperatures.

A vertical tubular furnace with a Kantal AF heater was used to carry out the experiments. The temperature was measured by an S-type thermocouple and controlled by a Eurotherm 818 P controller/programmer connected to a thyristor.

We mixed the chosen ratios of Gd_2O_3, K_2CO_3, and $NH_4H_2PO_4$ to prepare roughly 20 g of solution in a 25-cm^3 platinum crucible.

* To whom correspondence should be addressed. E-mail: aguilo@quimica.urv.es.

(1) Otsuka, K.; Yamada, T. *Appl. Phys. Lett.* **1975**, *26*, 311.
(2) Chinn, S. R.; Hong, H. Y.-P. *Appl. Phys. Lett.* **1975**, *26*, 649.
(3) Otsuka, K.; Yamada, T.; Saruwatari, M.; Kimura, T. *IEEE J. Quantum Electron.* **1975**, *QE11*, 330.
(4) Nakano, J.; Otsuka, K.; Yamada, T. *J. Appl. Phys.* **1976**, *47*, 2749.
(5) Hong, H. Y.-P. *Mater. Res. Bull.* **1975**, *10*, 1105.
(6) Otsuka, K.; Miyazawa, S.; Yamada, T.; Iwasaki, H.; Nakano, J. *J. Appl. Phys.* **1977**, *48*, 2099.
(7) Chinn, S. R.; Hong, H. Y.-P. *Opt. Commun.* **1975**, *15* (3), 345.
(8) Mazurak, Z.; Jezowska-Trzebiatkowska, B.; Schultze, D.; Waligora, C. *Cryst. Res. Technol.* **1984**, *19*, 7.
(9) Weber, H. P.; Damen, T. C.; Danielmeyer, H. G.; Tofield, B. C. *Appl. Phys. Lett.* **1973**, *22*, 534.
(10) Danielmeyer, H. G.; Huber, G.; Krühler, W. W.; Jeser, J. P. *Appl. Phys.* **1975**, *2*, 335.
(11) Chinn, S. R.; Pierce, J. W.; Heckscher, H. *IEEE J. Quantum Electron*. To be published.
(12) Parreu, I.; Solé, R.; Gavaldà, Jna.; Massons, J.; Díaz, F.; Aguiló, M. *Chem. Mater.* **2003**, *15*, 5059.
(13) Palkina, K. K.; Chudinova, N. N.; Litvin, B. N.; Vinogradova, N. V. *Izv. Akad. Nauk SSSR, Neorg. Mater.* **1981**, *17* (8), 1501.

10.1021/cm048442n CCC: $30.25
Published on Web 01/19/2005

Table 1. Growth Data Associated with KGP Single Crystals

expt	solution composition $Gd_2O_3-K_2O-P_2O_5$	solution wt (g)	seed orientation	seed position	cooling interval (K)	cryst dimens ($a \times b \times c$) (mm^3)	cryst wt (g)
1	4/31/65	20	a^*	centered	15	$1.4 \times 2.4 \times 1.8$	0.01
2	6/34/60	20	a^*	centered	15	$2.3 \times 6.7 \times 3.6$	0.13
3	6/34/60	20	a^*	acentered	15	$3.4 \times 7.1 \times 5.5$	0.29
4	6/34/60	200	a^*	acentered	20	$5.9 \times 15.6 \times 10.3$	1.77
5	6/34/60	200	b	acentered	20	$8.6 \times 4.8 \times 9.7$	1.63
6	6/34/60	200	c^*	acentered	20	$11.0 \times 16.2 \times 5.6$	1.94

These initial reagents were decomposed by heating them until the complete bubbling of NH_3, CO_2, and H_2O was reached. The solution was then homogenized by maintaining the temperature at about 50−100 K above the expected saturation temperature for 3−8 h, depending on the solution composition. The axial temperature gradient in the solution was about 10 K/mm and the surface was the coldest point of the whole volume.

We decreased the temperature of the homogeneous solution by 10 K approximately every 30 min until crystals appeared on a platinum wire immersed in the solution. The saturation temperature was then accurately determined by observing the growth or dissolution of these small crystals over long periods of time. Next, we used a platinum disk placed in contact with the solution surface and rotated it at 45 rpm to grow the crystals. The temperature was decreased to about 25 K below its saturation temperature at a cooling rate of 0.5−1 K/h to obtain the supersaturation of the solution.

We preliminarily identified the crystals by direct observation with an optical microscope and then by X-ray powder diffraction analysis. Some were also observed and photographed in a scanning electron microscope (SEM) JEOL JSM 6400.

X-ray Powder Diffraction. We used the X-ray powder diffraction technique to identify the KGP crystalline phase and some neighboring ones of the KGP crystallization region. The experiments were carried out with a D5000 Siemens X-ray powder diffractometer in a $\theta-\theta$ configuration using the Bragg−Brentano geometry and Cu Kα radiation. The X-ray powder diffraction patterns were recorded using a scintillation counter as detector.

Using this same equipment, we calculated the crystal cell parameters of KGP from the powder diffraction data obtained at 298 K in the 2θ range from 10 to 70°, using a step size of 0.03° and a step time of 5 s. To refine them, we used the structure of KNP previously solved[5,14] by single-crystal X-ray diffraction as the starting model.

We also used X-ray powder diffraction analysis to study how the crystal cell parameters evolved with temperature and to determine the thermal expansion tensor of KGP. We used the same equipment as before but with the addition of an Anton-Paar HTK10 platinum ribbon heating stage. The X-ray powder diffraction patterns were recorded at the same conditions: $2\theta = 10-70°$, step size = 0.03°, step time = 5 s, at temperatures of 298, 323, 373, 473, 573, 673, and 773 K, with a delay time of 300 s before each pattern recording.

We also analyzed the evolution of KGP with temperature in the room temperature to 1273 K range both by heating and cooling the sample. In this case, the X-ray powder diffractometer was equipped with the heating stage and also a Braun position-sensitive detector (PSD). The X-ray powder diffraction patterns were recorded at $2\theta = 10-70°$ and the measuring time per degree was 10 s. During the heating cycle, the sample was heated at a rate of 10 K/s from room temperature to 673 K and from this point to the maximum (1273 K) it was heated at a lower rate of 0.17 K/s. The cooling cycle was designed using the same conditions. Diffraction patterns were registered every 50 K between 673 and 1273 K in both processes.

Differential Thermal Analysis (DTA). We also used DTA measurements to study the evolution of KGP with temperature before analyzing it more accurately by X-ray powder diffraction. This analysis was carried out in a TA Instruments simultaneous differential techniques instrument SDT 2960. We used calcined Al_2O_3 as reference material and Ar, at a flow of 90 cm^3/min, as purge gas. The powdered sample, which weighed around 20 mg, was placed in a platinum pan and heated at a rate of 10 K/min between room temperature and 1273 K. The storage rate of data was 0.5 s/data point.

Top-Seeded Solution Growth (TSSG). We used the top-seeded solution growth (TSSG) slow cooling method without pulling to obtain inclusion-free KGP single crystals of a suitable size for later studies. We performed the growth experiments using a vertical furnace controlled by a Eurotherm 818 P controller/programmer. A conical platinum crucible was used to contain the solution, the homogenization of which was achieved by keeping the temperature about 50 K above the expected saturation temperature for 3−4 h. The solution surface was the coldest point of the whole volume and the temperature gradient in its axial direction was 1.2 K/mm. We accurately determined the saturation temperature by observing the growth or dissolution of a seed in contact with the solution surface. Then, when the solution temperature was decreased at a rate of 0.1 K/h, the crystal began to grow completely submerged in the solution on the seed bottom, which was constantly rotated during the growth process at 75 rpm. We used parallelepipedic oriented seeds of similar size for all experiments. These were around 8 mm along the axial direction (a^*, b, or c^*) of the rotation movement and around 2 mm in the other two radial directions. After the temperature was decreased by the chosen interval (15 or 20 K) the crystal was slowly removed from the solution and then cooled to room temperature at 30 K/h.

To optimize the crystal growth process, we performed several experiments under conditions chosen by taking into account the results of the previous study on KNP.[12] The cooling rate and rotation velocity were thus kept constant at 0.1 K/h and 75 rpm because the viscosities of the two solutions were similar. We analyzed how the solution composition and seed orientation affected the KGP crystal growth (see Table 1 for values and corresponding results). We evaluated these results by taking into account the growth rate and quality of the KGP crystal grown.

First we filled a platinum conical crucible of 25 cm^3 with suitable amounts of reagents to prepare roughly 20 g of solution with the compositions shown in Table 1 (experiments 1 and 2) to study the effect of solution composition. With this lower amount of solution we also checked the suitability of using the previously introduced growth device.[12] In this case it also improved both crystal quality and growth rate (experiment 3). This growth device comprises a platinum turbine centered on the rotation axis and a seed support above it displaced around 11 mm from this axis. The effect of seed orientation was then analyzed using a larger amount of solution (around 200 g) placed in a platinum crucible of 125 cm^3. The seeds used were as described above (experiments 4−6).

(14) Parreu, I.; Solans, X.; Aguiló, M. Unpublished.

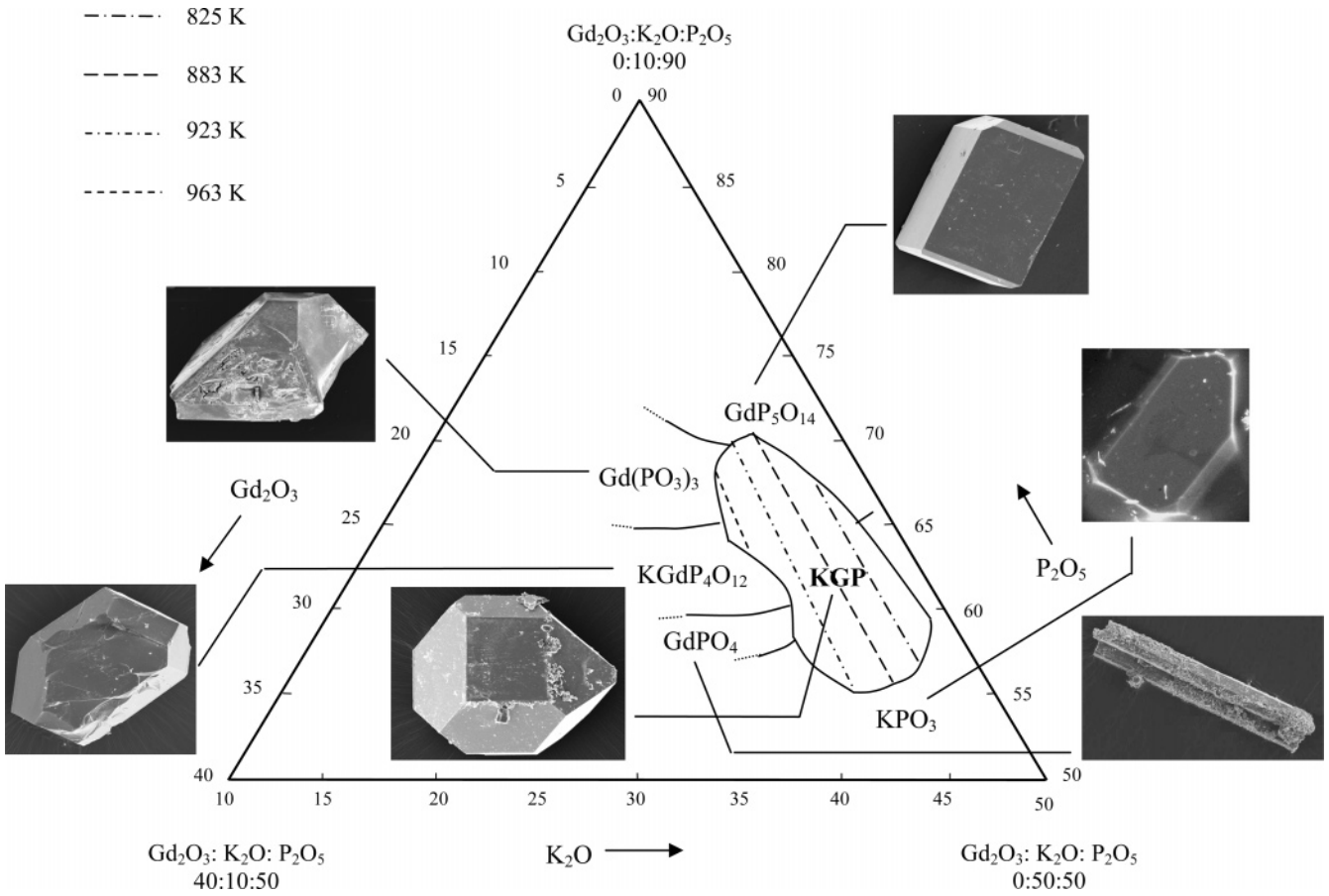

Figure 1. Crystallization Region of KGP and saturation temperatures in the $Gd_2O_3-K_2O-P_2O_5$ system. SEM images of KGP and neighboring phases.

Second Harmonic Generation (SHG) Measurements. We evaluated the second harmonic response of KGP using the Kurtz method.[15] Small KGP crystals were powdered and graded with standard sieves to obtain a uniform particle size between 5 and 20 μm, and then uniformly packed. The sample was then placed in a 2-mm-thick quartz cell and irradiated using a pulsed Nd:YAG laser.

To estimate the incident power, we measured the energy reflected by the sample. We also measured the energy of the double radiation it emitted, the frequency of which was twice that of the incident radiation, using a silicon PIN. We used the ratio between these signals, calculated as an average of over 100 laser shots, to estimate the second harmonic efficiency of the sample and compared this efficiency with that of KDP,[16] which is a well-known nonlinear optical material.

Results and Discussion

KGP Crystallization Region. Figure 1 shows the crystallization region of KGP in the $Gd_2O_3-K_2O-P_2O_5$ ternary system and the saturation temperature isotherms determined after studying about 50 solution compositions. SEM images of KGP and neighboring phases are added.

In general, polyphosphates have many local geometries—long-chains or cycles—and crystalline structures, because when they are formed the phosphate units have a high versatility of condensation. The structure of those of lanthanides is highly dependent on the size of this ion. From this point of view, two groups are defined, one for ions belonging to the first half of lanthanides and one for ions belonging to the second half. Since gadolinium is placed just in the middle, $KGd(PO_3)_4$ can present the phase presented and named by us as KGP (monoclinic, $P2_1$, $a = 7.2701(11)$ Å, $b = 8.3818(8)$ Å, $c = 7.9608(10)$ Å, $\beta = 91.776(12)°$, $Z = 2$, and $V = 484.87(11)$ Å^3) usual for the first half, and the usual for the second half (monoclinic, $P2_1/n$, $a = 10.412(2)$ Å, $b = 8.996(2)$ Å, $c = 10.836(2)$ Å, $\beta = 105.94(1)°$, $Z = 4$, and $V = 975.9(3)$ Å^3).[17] Studying the KGP crystallization region, we found that the neighboring phase $Gd(PO_3)_3$ also presented polymorphism in most of the compositions we studied—a mixture of the orthorhombic phase (first half) and the monoclinic one (second half).

The high versatility would explain the irregularity of the KGP crystallization region and the many neighboring phases around it, among which we also found the polymorph phase of KGP in a cycling geometry, $KGdP_4O_{12}$. In Table 2, therefore, we summarize the composition limits of the KGP crystallization region and the neighboring phases determined. The limit points are defined by the intersection of the Gd_2O_3/K_2O isoconcentrational lines with P_2O_5 molar concentrations. The isoconcentrational lines of this ratio are roughly parallel to the saturation temperature isotherms whcih increase from 825 to 963 K when the Gd_2O_3/K_2O ratio is also increased. KGP crystallizes inside these points (Table 2) and up to a Gd_2O_3/K_2O ratio of 3/97 and P_2O_5 concentration approximately between 58 and 65. The six neighboring phases

(15) Kurtz, S. K.; Perry, T. T. *J. Appl. Phys.* **1968**, *39*, 3798.
(16) Dmitriev, V. G.; Gurzadyan, G. G.; Nikogosyan, D. N. *Handbook of Nonlinear Optical Crystals*; Springer-Verlag: New York, 1991.
(17) Rekik, W.; Naïli, H.; Mhiri, T. *Inorg. Acta Crystallogr.* **2004**, *C60*, i50.

Table 2. Solution Composition Limits of the KGP Crystallization Region and the Neighboring Crystalline Phases Determined

solution composition (mol %)		
molar ratio Gd_2O_3/K_2O	P_2O_5 mol %	neighboring phase
5/95	57	KPO_3
5/95	67	GdP_5O_{14}
10/90	56	KPO_3
10/90	71	GdP_5O_{14}
15/85	55	KPO_3
15/85	70	GdP_5O_{14}
20/80	58	$GdPO_4$
20/80	64	$KGdP_4O_{12}$
20/80	68	$Gd(PO_3)_3$

identified are KPO_3, $GdPO_4$,[18] $KGdP_4O_{12}$,[19] $Gd(PO_3)_3$-orthorhombic,[20] $Gd(PO_3)_3$-monoclinic,[20] and GdP_5O_{14}.[21] While KPO_3 crystallizes below the crystallization region, GdP_5O_{14} crystallizes above it. In the same P_2O_5 concentration range as the crystallization region, but in the highest Gd_2O_3 concentration zone, the other phases—$GdPO_4$, $KGdP_4O_{12}$, and orthorhombic and monoclinic $Gd(PO_3)_3$—crystallize.

The viscosity of the solutions was quite high, though varied, throughout the crystallization region. Crystal growth is very difficult in highly viscous solutions because, due to the low molecular mobility inside them, the growth units find it difficult to reach the crystal surface. The average growth rate and the crystal quality therefore decrease and the average time of homogenization increases. So we qualitatively studied the relationship between the solution composition and the growth rate, which is directly influenced by the viscosity of the solution. When we increased the P_2O_5 concentration and kept the Gd_2O_3/K_2O ratio constant, the viscosity went up. The viscosity also went up when we decreased this Gd_2O_3/K_2O ratio, probably because the saturation temperature also decreased, taking into account the inverse relationship between viscosity and temperature. When the K_2O concentration was above 98 mol %, the increase in solution viscosity hindered crystallization at all P_2O_5 concentrations.

Using these results, we chose an apparently optimal composition zone to initiate the growth experiments of KGP single crystals. This is the zone with a low P_2O_5 concentration and fairly displaced to the left corner, where the saturation temperature is highest and the K_2O concentration is lowest.

Top-Seeded Solution Growth (TSSG) of KGP Single Crystals. We analyzed how solution composition and seed orientation affected the growth rate and quality of KGP single crystals. The conditions and results of the experiments are shown in Table 1. For all of these experiments, the rotation velocity was 75 rpm and the cooling rate was 0.1 K/h.

To check how viscosity affected the crystal growth process, we chose $Gd_2O_3-K_2O-P_2O_5 = 4/31/65$ mol % (experiment 1) that was fairly displaced from the optimal composition zone previously determined because of the high P_2O_5 concentration. The crystals obtained from this solution were too small and too light, despite the long cooling period, and their quality was also very low. The composition of the solution for growing KGP single crystals should therefore be chosen from the optimal zone determined. We used $Gd_2O_3-K_2O-P_2O_5 = 6/34/60$ mol % placed in this zone to grow the crystals, the optimal value for KNP.[12]

We also checked the use of the previously described growth device. Its platinum turbine increased the movement of the growth units inside the solution, which had been hindered by the viscosity. As with KNP,[12] this device increased both the growth rate and the quality of the crystals (experiment 3).

KGP crystal growth was achieved using the three crystallographic directions, *a**, *b*, and *c**, as axial seed orientation. Although the quality of the crystals was quite similar, there were some differences in growth rate. The lowest growth rate was for the *b* seed orientation. For the other two orientations (experiments 4−6), the growth rates were similar. Figure 2a shows a KGP single-crystal grown in experiment 4.

Crystal Structure of KGP. We calculated the crystal cell parameters of KGP from the X-ray powder diffraction data using the FULLPROF program[22] and the Rietveld method.[23] The structure of KNP, solved earlier[5,14] by single-crystal X-ray diffraction, was used as the starting model. We selected a Pearson VII function and included in the final Rietveld refinement the following parameters: zero-point, scale factor, background coefficients, the four cell parameters (a, b, c, and β), and one profile shape parameter. We determined the following: $a = 7.2701(11)$ Å, $b = 8.3818(8)$ Å, $c = 7.9608(10)$ Å, $\beta = 91.776(12)°$, $V = 484.87(11)$Å^3, $P2_1$, and $Z = 2$. The cell parameters were slightly smaller than those for KNP because the ionic radius for Gd^{3+} is slightly smaller than that for Nd^{3+} (0.938 Å and 0.995 Å, respectively).

Crystal Morphology of KGP. We observed small KGP single crystals by scanning electron microscopy (SEM) (Figure 1) and large ones using an optical microscope (Figure 2a) to describe its morphology. The habit was made up of the crystalline forms {001}, {100}, {011}, {0$\bar{1}$1}, {110}, {1$\bar{1}$0}, {10$\bar{1}$}, {101}, {1$\bar{1}\bar{1}$}, and {111}. Figure 2b shows the theoretical model, made with the Shape software,[24] in which most faces are hexagonal or square. Many of these faces are not equivalent by symmetry but are very similar since the β angle of KGP is close to 90° and its cell parameters are quite similar, which recommends using X-ray diffraction techniques in face indexation.

Linear Thermal Expansion Tensor. As some of the pumping light power is converted into heat inside KGP, we determined and located its thermal ellipsoid in order to determine how the temperature affected its structure. We analyzed the X-ray powder diffraction patterns in the 298−773 K temperature range using the FULLPROF program[22] and the Rietveld method[23] to determine how the cell

(18) Mullica, D. F.; Grossie, D. A.; Boatner, L. A. *Inorg. Chim. Acta* **1985**, *109*, 105.
(19) Ettis, H.; Naïli, H.; Mhiri, T. *Cryst. Growth Des.* **2003**, *3* (4), 599.
(20) Mel'nikov, P. P.; Komissarova, L. N.; Butuzova, T. A. *Izv. Akad. Nauk SSSR, Neorg. Mater.* **1981**, *17* (11), 2110.
(21) Bagieu-Beucher, M.; Duc, T. Q. *Bull. Soc. Fr. Mineral Crystallogr.* **1970**, *93*, 505.
(22) Rodríguez-Carvajal, J. *Short Reference Guide of the Computer Program FULLPROF*; Laboratoire León Brillouin, CEA-CNRS: Saclay, France, 1998.
(23) Young, R. A., Ed. *The Rietveld Method*; Oxford Science Publication-;International Union of Crystallography: Chester, U. K., 1995.
(24) Dowty, E. *Shape for Windows*, version 5.0.1; 1995.

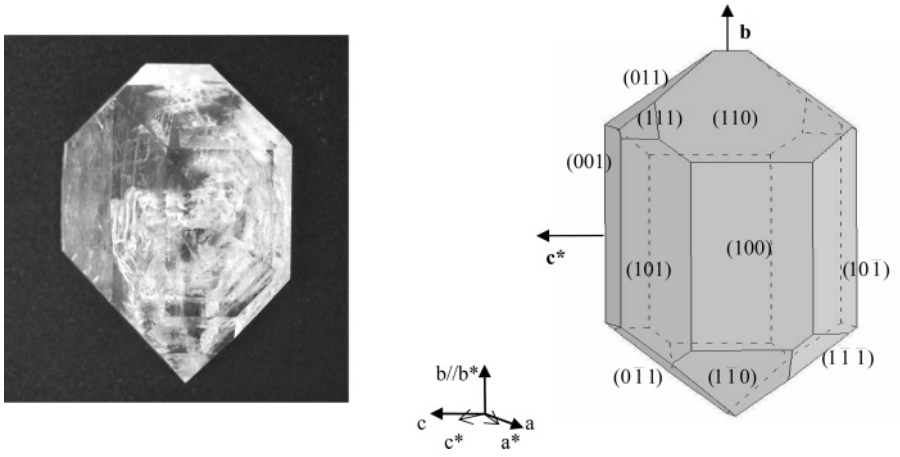

Figure 2. (a) KGP single-crystal grown with a seed in the *a** direction. (b) Scheme of the crystal morphology.

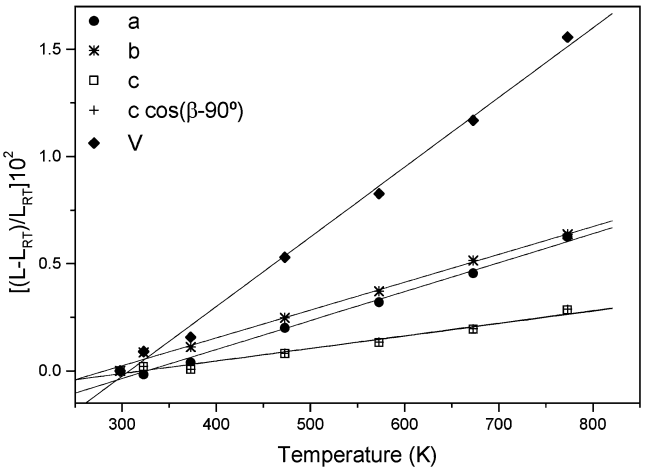

Figure 3. Relative thermal evolution of the cell parameters and unit cell volume of the $KGd(PO_3)_4$.

parameters evolved with temperature. The linear relationship between the average change in each cell parameter ($\Delta L/L$) and temperature is shown in Figure 3. As the temperature increased, KGP dilated slightly. While the β angle remained roughly constant, the cell parameters *a*, *b*, and *c* all increased in a similar way. This almost isotropic thermal expansion is a good property that prevents KGP from deforming when it is working above room temperature.

The linear thermal expansion coefficients can be calculated from the slope of the linear relationship ($\Delta L/L$) and the temperature for each unit cell parameter. The linear thermal expansion tensor at room temperature in the crystallophysical system $X_1||a$, $X_2||b$, $X_3||c^*$ is

$$\alpha_{ij(\mathrm{KGP})} = \begin{pmatrix} 13.50 & 0 & 0.60 \\ 0 & 13.00 & 0 \\ 0.60 & 0 & 5.86 \end{pmatrix} \times 10^{-6}\,\mathrm{K}^{-1}$$

In the principal system X_1',$X_2'||b$, X_3', the diagonalized linear thermal expansion tensor is

$$\alpha'_{ij\ (\mathrm{KGP})} = \begin{pmatrix} 13.55 & 0 & 0 \\ 0 & 13.00 & 0 \\ 0 & 0 & 5.81 \end{pmatrix} \times 10^{-6}\,\mathrm{K}^{-1}$$

The principal axis, X_1', was found 4.76° clockwise from the *a* axis. The axis with a minimum thermal expansion, X_3', was found 2.69° from the *c* axis. The thermal expansion ellipsoid in the principal axes is shown in Figure 4.

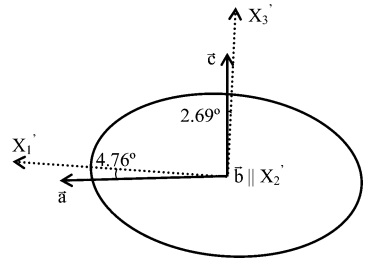

Figure 4. Thermal expansion ellipsoid for KGP in projection parallel to [010].

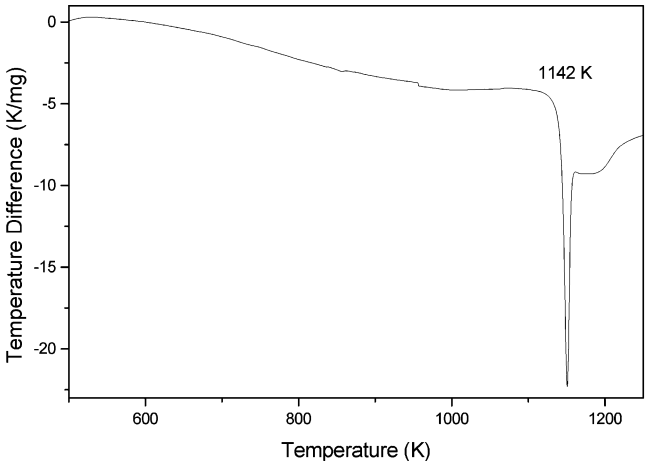

Figure 5. Differential thermal analysis (DTA) thermogram of $KGd(PO_3)_4$ in the 573−1273 K temperature range.

Phase Transitions. We analyzed how KGP evolved with temperature between room temperature and 1273 K using differential thermal analysis (DTA) and X-ray powder diffraction. Using DTA, we determined the exothermic transformation suffered by KGP at 1142 K. Figure 5 shows the thermogram obtained during the heating process in the 500−1250 K range. The change in weight during the experiment was not representative.

We studied this transformation more accurately by X-ray powder diffraction and identified the crystal phases involved. The bottom of Figure 6 shows the X-ray powder diffraction pattern of $KGd(PO_3)_4$ at room temperature and the selected

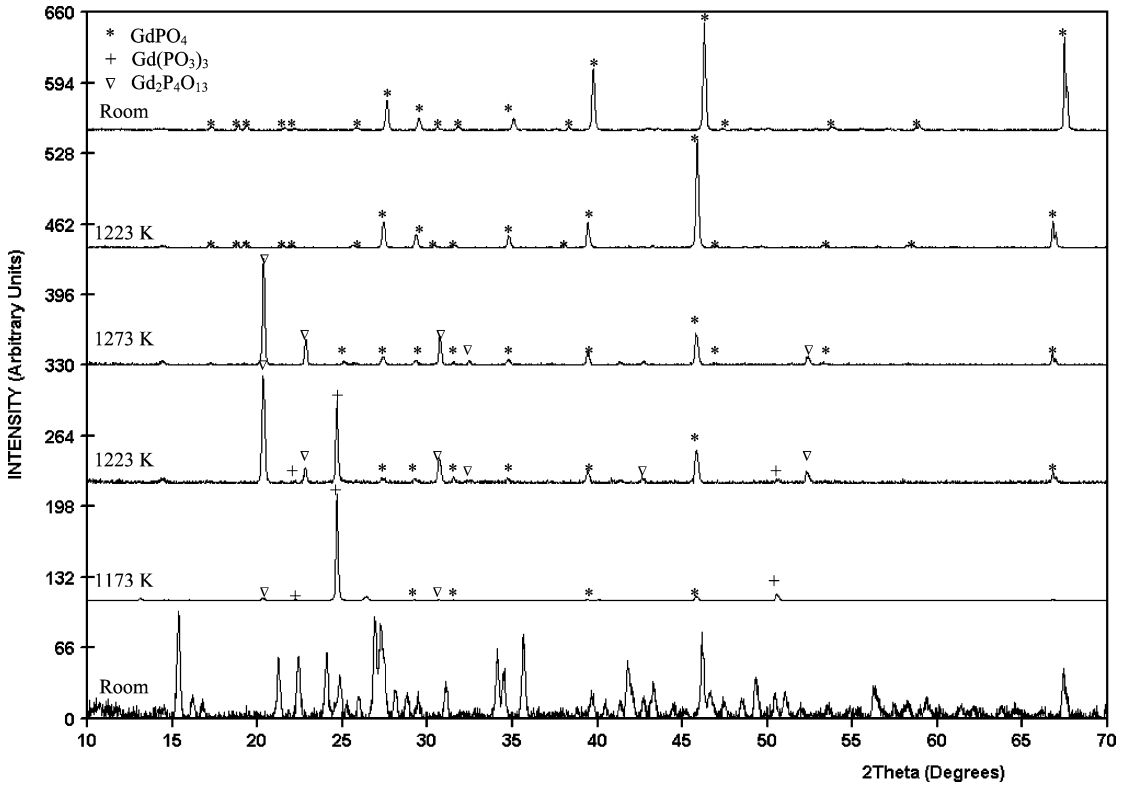

Figure 6. X-ray powder diffraction pattern of $KGd(PO_3)_4$ at room temperature and the selected patterns at several temperatures describing the evolution of $KGd(PO_3)_4$ with temperature in both the heating and cooling processes.

patterns at several temperatures which describes its evolution in both the heating and the cooling processes. The three new crystalline phases were identified as $GdPO_4$ (83-0657 ICDD database[18]), $Gd(PO_3)_3$ (the orthorhombic form, which is isostructural to that of the EuP_3O_9 31-0519 ICDD database[25]), and $Gd_2P_4O_{13}$ (35-0078 ICDD database[26]). Though all appeared in the X-ray diffraction pattern recorded at 1173 K, they behaved differently since only $GdPO_4$ remained until room temperature. $Gd(PO_3)_3$ appeared as the predominant phase at 1173 K but the intensity of its peaks rapidly decreased between this temperature and 1273 K, when it completely disappeared. As the intensity of the $Gd(PO_3)_3$ peaks decreased, the intensity of the peaks for the other two phases increased steadily in the same temperature range. At 1223 K during the cooling process $Gd_2P_4O_{13}$ completely disappeared and $GdPO_4$ became the only phase. From this temperature, the intensity of the $GdPO_4$ peaks remained fairly constant until room temperature. A slight displacement of the peaks was observed in the last X-ray diffractogram at room temperature because of the dilation of the material.

The X-ray powder diffraction study showed that KGP decomposed at 1173 K into GdPO4, $Gd(PO_3)_3$, $Gd_2P_4O_{13}$, and an amorphous phase, which probably contained phosphorus and potassium oxides because the sample weight remained roughly constant. However, between this temperature and 1223 K during the cooling process, a completely crystalline transformation of $Gd(PO_3)_3$ and $Gd_2P_4O_{13}$ into $GdPO_4$ occurred which probably involved a loss of amorphous potassium oxide. The $Gd(PO_3)_3$ transformation was completed first (at 1273 K) and the $Gd_2P_4O_{13}$ transformation was completed at 1223 K cooling process. The exothermic peak observed in the thermogram at 1142 K may be related to this decomposition.

These results therefore suggest that KGP decomposes irreversibly at 1142 K in accordance with this reaction:

$$4KGd(PO_3)_4 \rightarrow Gd(PO_3)_3 + GdPO_4 + Gd_2P_4O_{13} + \text{amorphous phase}$$

Second Harmonic Generation. The SHG efficiency (η) of KNP, calculated as previously described, was compared with the efficiency of KDP, which is widely used for nonlinear optical applications. The value of η/η_{KDP} we obtained was approximately one. The possibility of developing a self-frequency doubling laser increases interest in this material.

Conclusions

We determined the crystallization region of $KGd(PO_3)_4$ in the $Gd_2O_3-K_2O-P_2O_5$ system with its saturation temperature isotherms. We proved that solution compositions chosen from the optimal zone determined were suitable to grow single crystals. This zone is poor in P_2O_5 and rich in Gd_2O_3 and saturation temperatures related are the highest. We successfully grew KGP single crystals by the top-seeded solution growth-slow cooling method (TSSG). To achieve a suitable quality and size of crystals for later studies, several crystal growth conditions were optimized. We conclude that all three seed orientations are suitable for growing KGP by TSSG. Our results were similar when we used *a** or *c** orientations but the growth rate slightly decreased when we

(25) Tsujimoto, Y. *J. Electrochem. Soc.* **1977**, *124*, 553.

(26) Agrawal, D.; Hummel, J. *J. Electrochem. Soc.* **1980**, *127*, 1550.

used the *b* orientation. The suitability of the growth device was also proved.

KGP dilates slightly in any crystallographic direction and in an almost isotropic way. It decomposes irreversibly at 1142 K according to the reaction proposed and between this temperature and 1223 K crystalline transformations occur to finally generate a single product, $GdPO_4$, at room temperature.

Finally, we found that the second harmonic efficiency of KGP was similar to that of KDP.

Acknowledgment. We acknowledge financial support from DURSI 2001SGR317 and 2003FI00770 and CICyT MAT-02-04603-C05-03 and FIT070000-2003-661.

CM048442N